Tailoring the flow properties of inhaled micronized drug powders by atomic and molecular layer deposition

Zhang, Fuweng; Wu, Kaiqiao; La Zara, Damiano; Sun, Feilong; Quayle, Michael J.; Petersson, Gunilla; Folestad, Staffan; Chew, Jia Wei; van Ommen, J. Ruud

Important note
To cite this publication, please use the final published version (if applicable).
Please check the document version above.

Tailoring the flow properties of inhaled micronized drug powders by atomic and molecular layer deposition

Fuweng Zhang [a,b,*], Kaiqiao Wu [b], Damiano La Zara [b], Feilong Sun [b], Michael J. Quayle [c], Gunilla Petersson [d], Staffan Folestad [d], Jia Wei Chew [e], J. Ruud van Ommen [b,*]

[a] Qingyuan Innovation Laboratory, Quanzhou 362801, China
[b] Department of Chemical Engineering, Delft University of Technology, Van der Maasweg 9, Delft 2629 HZ, the Netherlands
[c] Oral Product Development, Pharmaceutical Technology & Development, Operations, AstraZeneca Gothenburg, Sweden
[d] Innovation Strategy and External Liaison, Pharmaceutical Technology & Development, Operations, AstraZeneca, Gothenburg, Sweden
[e] School of Chemical and Biomedical Engineering, Nanyang Technological University, 637459, Singapore

ARTICLE INFO

ABSTRACT

For dry powder inhaled formulations, good flow behaviour is vital in re-dispersing the powder. However, inhaled drug powders with a particle size below 10 μm are classified as highly cohesive materials with poor flow characteristics. Here we demonstrate how to alter the flow properties of micronized budesonide powders by depositing different materials (organic, inorganic, and hybrid organic–inorganic) in the forms of nanoscale films onto the drug particles using atomic/molecular layer deposition (ALD/MLD) coatings. The angle of repose (static) and pneumatic delivery measurements were performed to access the flow characteristics. The flowability can be effectively improved with the growth of inorganic nanofilm (SiO_2, TiO_2, or Al_2O_3) via ALD and hybrid nanofilm (titanicone) via combined ALD-MLD coating. This improvement is reflected by the decrease in the angle of repose and minimum pick-up velocity (U_{pu}), as well as promoting the pneumatic delivery of a much larger amount of drug powders after ALD or hybrid coating. In contrast, the organic PET coated budesonide via MLD exhibits comparable poor flow characteristics as the uncoated budesonide. Rather than being transported in individual particles, the uncoated or PET-coated budesonide powders are pneumatically delivered in form of complex clusters with a size of over 500 μm, whereas the ALD budesonide is dispersed in form of small agglomerates (<100 μm). Despite the difference in agglomerate size, entraining behaviors of all samples agree well with the prediction of Kalman's pick-up Zone I correlation. The inorganic nanofilm deposited via ALD alters the surface chemistry to reduce the inter-particle forces measured by atomic force microscopy, giving rise to an improved drug delivery performance. Nanoscale surface modification of dry powder particles has good potential for inhaled drug delivery enhancement.

1. Introduction

Powder materials as ingredients or products are widely used in many applications, such as chemical, cosmetic, food, and pharmaceutical industries. One of the main physical properties of powders is their flow characteristic which has a significant influence on manufacturing efficiency and product quality attributes such as content uniformity. To satisfy manufacturing demands and ensure the accuracy and uniformity of pharmaceutical dosage forms, good powder flow is needed [1,2]. In particular, flowability plays an important role in drug delivery performance when pharmaceuticals are administered as a powder from dry powder inhaler (DPI) systems [3]. Good flow behavior of pharmaceutical powders is vital in the re-dispersion of powder in inhalers. However, low-micron-sized drug powders generally exhibit poor flow behavior which depresses consistent drug delivery. This is due to the inter-particle cohesive forces which play a dominant role in the bulk powder behavior when the individual particles are smaller than 30 μm. Therefore, modifying the flow characteristic of inhalation drugs is very

beneficial for improving drug delivery performance.

Surface modification with dry particle coatings [4–6] offers the potential to control and tailor the properties of the target materials. Different from the conventional dry coating methods, atomic layer deposition (ALD) is a vapor deposition technique where an ultrathin film grows by sequential exposure of gas-phase reactants onto the target material with atomic layer accuracy [7–9]. Due to the advantages of excellent conformality and film thickness control at the atomic level, ALD offers the possibility of coating primary particles as well as complex structures with a large surface area to functionalize the surface properties of targeted materials for improving different product performances [10–16], such as modifications of wetting [17], acid-base [18], optical, mechanical and rheological properties [19–21]. Although ALD is popular among the scientific community for modifying the surface properties of materials, this technique has been mainly used on flat substrates or fibers [22–24]. Especially, so far only very few attempts have been made to modify the flow characteristics of particulate materials via ALD. Hirschberg et al. reported that depositing a thin layer of TiO_2 by ALD on the host particle surface can quadruple the flowability of a partially crystalline material and triple the flowability of an amorphous material [10]. Hakim et al. [19] found that the growth of ultrathin alumina (Al_2O_3) films via ALD on primary titania nanoparticles with an average size of 21 nm can effectively decrease the viscosity of the particle assembly and, therefore, alter the rheological property. The improvements in powder flow can also be achieved by coating polymer powder feedstocks with aluminum oxide (Al_2O_3) using ALD, attributed to the decrease in the surface energy after coating treatment [21]. ALD coating using metal oxides such as Al_2O_3 and TiO_2 on active pharmaceutical ingredients (APIs), can reduce the electrostatic charge build-up of the drug particles without affecting their physicochemical properties [25]. Nevertheless, those studies were all focused on growing inorganic film to modify the powder flow, how the organic or hybrid inorganic–organic nanocoatings affect the flow properties of host powders still remains unknown.

Atomic layer deposition (ALD) is developed to make high-quality conformal inorganic thin coatings, while molecular layer deposition (MLD) is its less-exploited counterpart for purely organic thin coatings. The hybrid inorganic–organic coatings obtained by combining ALD and MLD, may not only possess properties combined with those of the two parent materials, but may also have completely new material properties. However, compared to inorganic coatings, organic or hybrid coatings would encounter various difficulties when using organic precursors. Organic precursor molecules with long chains are likely to tilt such that the growth is not perfectly perpendicular to the surface. Likewise, organic molecules may bend and react twice with the surface, reducing the number of reactive surface sites and lowering the growth rate. Organic precursors are also often bulky, causing steric hindrance [26]. In this work, we demonstrate surface modification by depositing inorganic, organic, and hybrid inorganic–organic nanoscale films by ALD and MLD to tune the flow characteristics of low micronized budesonide drug powders with special focus on 2–5 μm. Inorganic oxide ceramic shells of SiO_2, TiO_2, and Al_2O_3 were grown on the surface of budesonide particles via ALD coating. Nanoscale films of PET (polyethylene terephthalate) were deposited onto budesonide via MLD which can be seen as the organic version of ALD. The two techniques can also be combined to fabricate hybrid inorganic–organic materials. Titanicone films were synthesized via $TiCl_4$/ethylene glycol hybrid ALD/MLD. To enable optimization of the drug delivery performance, the effect of different coating materials on the flow behavior of inhalation budesonide powders characterized by the angle of repose (static) and pneumatic transportation (dynamic) tests were investigated.

2. Materials and methods

2.1. Materials

Budesonide pharmaceutical powder was used as the substrate material. It is an anti-inflammatory corticosteroid compound and is used to treat asthma or chronic obstructive pulmonary disease by respiratory inhalation [27–29]. Micronized budesonide powder with a particle size distribution of 0.1 to 10 μm was used. Different precursors were used to deposit the desired coating films on the surfaces of budesonide particles. For inorganic ALD coatings of silica, titanium, and alumina, the metal precursors ($SiCl_4$, $TiCl_4$, and trimethylaluminum, TMA) and co-reactants (demineralized water or ozone) contained in stainless steel bubblers were used. However, instead of using metal precursors, the organic MLD coating of PET (polyethylene terephthalate) on budesonide was obtained by using terephthaloyl chloride (TC) and ethylene glycol (EG). The titanium tetrachloride ($TiCl_4$) based on the combination of an organic compound, EG was used to deposit the hybrid inorganic–organic titanicone films by the combined ALD/MLD coating.

2.2. Fluidized bed ALD/MLD coatings on budesonide

ALD/MLD or hybrid coating experiments were carried out in a vibrated fluidized bed reactor operating at atmospheric pressure. A similar setup can be found in the former works of Zhang and La Zara et al. [14,16,17]. The reaction chamber consists of a glass column (26 mm in internal diameter and 500 mm in height). For each test, powder samples were loaded into the column and placed on a single motor Paja PTL 40/40–24 vertical vibration table to assist the fluidization.

Depending on the deposited materials needed, different combinations of precursors used were contained in stainless steel bubblers kept at room temperature. The stainless steel tubing connecting the bubblers and the reactor was maintained at 30 °C above the bubblers' temperature to avoid precursor condensation. The reactor was heated by an infrared lamp placed parallel to the column with feedback control to maintain a constant operating temperature during the coating process. The precursor and co-reactant vapors were transported to the reactor column using an inert gas flow (N_2, 99.999 v/v%) which acts as a carrier and purging gas. A similar coating process based on sequential self-limiting surface reactions between gaseous precursors and a solid substrate is used for either ALD, MLD, or the combined ALD/MLD process. First, reactant A is fed to the reactor and reacts with the functional groups on the drug particle surface. Then, reactant B is fed to the reactor and reacts with the chemisorbed reactant A and forms the desired material. These two steps are separated by purging steps to remove unreacted species. The steps above constitute 1 process cycle. By repeating these cycles, the films of the desired thickness with atomic-level accuracy grow on the surface of host budesonide particles. A summary of the coating experiments (precursors and their exposure times in each deposition process) is presented in Table 1. In specific, the precursors (TMA, $TiCl_4$, and $SiCl_4$) and co-reactants (O_3 and H_2O) were kept at room temperature for the ALD process, whereas the precursors (TC and EG) were heated to 100 °C for the MLD process. The operating temperature of the reactor was set at 40 °C, 150 °C, and 120 °C for ALD, MLD, and ALD/MLD experiments, respectively. 5 g of budesonide powder batches were loaded into the reactor for the ALD and MLD experiments, whereas 8 g were used in the hybrid ALD/MLD experiment. Optimized gas flows of 1 L/min, corresponding to 3.4 cm/s at room temperature, for 5 g of budesonide and 2 L/min, corresponding to 6.7 cm/s at room temperature, for 8 g of budesonide were employed to deliver the precursors to the reactor and sufficiently fluidize the powder with the assistance of mechanical vibration. ALD of SiO_2, Al_2O_3, and TiO_2 and hybrid ALD/MLD of titanicone were run for 10 cycles, whereas MLD of PET was for 50 cycles.

Table 1
Overview of operating conditions for the ALD/MLD experiments.

Film type	Coating process	Deposited films	Reactant A (T, °C)	Reactant B (T, °C)	$T_{reaction}$ (°C)	Exposure time (min) (Precursor-N$_2$-Coreactant-N$_2$)	Coating cycles
Inorganic	ALD	Al_2O_3	TMA (30 °C)	O_3	40	1–5–1–5	10
		SiO_2	$TiCl_4$ (R_T)	H_2O	40	0.5–5–1–5	10
		TiO_2	$SiCl_4$ (R_T)	H_2O	40	0.25–5–1–5	10
Organic	MLD	PET	TC (100 °C)	EG	150	1–5–1–5	50
Hybrid Inorganic-Organic	Combined ALD/MLD	Titanicone	$SiCl_4$ (R_T)	EG	120	0.5–2–1.5–10	10

2.3. Surface characterization by transmission electron microscopy (TEM)

The conformality of the ALD/MLD coating was investigated via transmission electron microscopy (TE). The particles were suspended in ethanol and transferred to regular TEM grids (3.05 mm in diameter). TEM images were taken using a JEOL JEM1400 operating at 120 kV. The TEM images were then analyzed using the software package ImageJ to determine the thickness of the inorganic, organic, and hybrid inorganic–organic films.

2.4. Angle of repose measurement

The angle of repose (AOR) is a static characterization of powder flowability, significantly affected by particle shape and size, moisture content, bulk density, and the action of gravity. Whereas, mass loss during pneumatic entrainment indicates the dynamic properties of powder flow. The flowability characteristic of powder material is directly related to both the physical properties of the material itself, as well as the specific processing conditions in the handling system. Consequently, for such a complex system, a single measurement used to describe powder flowability may not provide sufficient information. Therefore, Both the angle of repose (static) and pneumatic trans-

portation (dynamic) tests were employed to investigate the flowability of drug powders used in this work. The angle of repose of the powders (AOR) was measured according to the Hosokawa powder testing method [30,31] and was used as an indicator of flowability. A funnel was held 4 cm above the flat base while the powder samples were poured through it. The AOR is defined as the angle between the surface of the powder heap and the surface of the plate. The diameter and the height of the powder's heap formed at the surface were measured and the static angle of repose (a) was calculated using $a = \tan^{-1}\left(\frac{2h}{D}\right)$, where h is the height and D is the diameter of the conical heap formed. The same test was repeated 3 times for each powder sample and the mean value was considered as the AOR. Generally, a smaller value of AOR stands for better flowability. When AOR is <30°, the flowability is said to be excellent; on the other hand, if AOR is greater than 45°, the flowability is considered poor [32].

2.5. Characterization of particles' pick-up behavior

The schematic of the pneumatic delivery setup for characterizing the flow behavior of uncoated and coated budesonide is similar to that in studies of Anantharaman et al. [33–36], illustrated in Fig. 1. The setup consisted of three cylindrical sections with a consistent inner diameter of
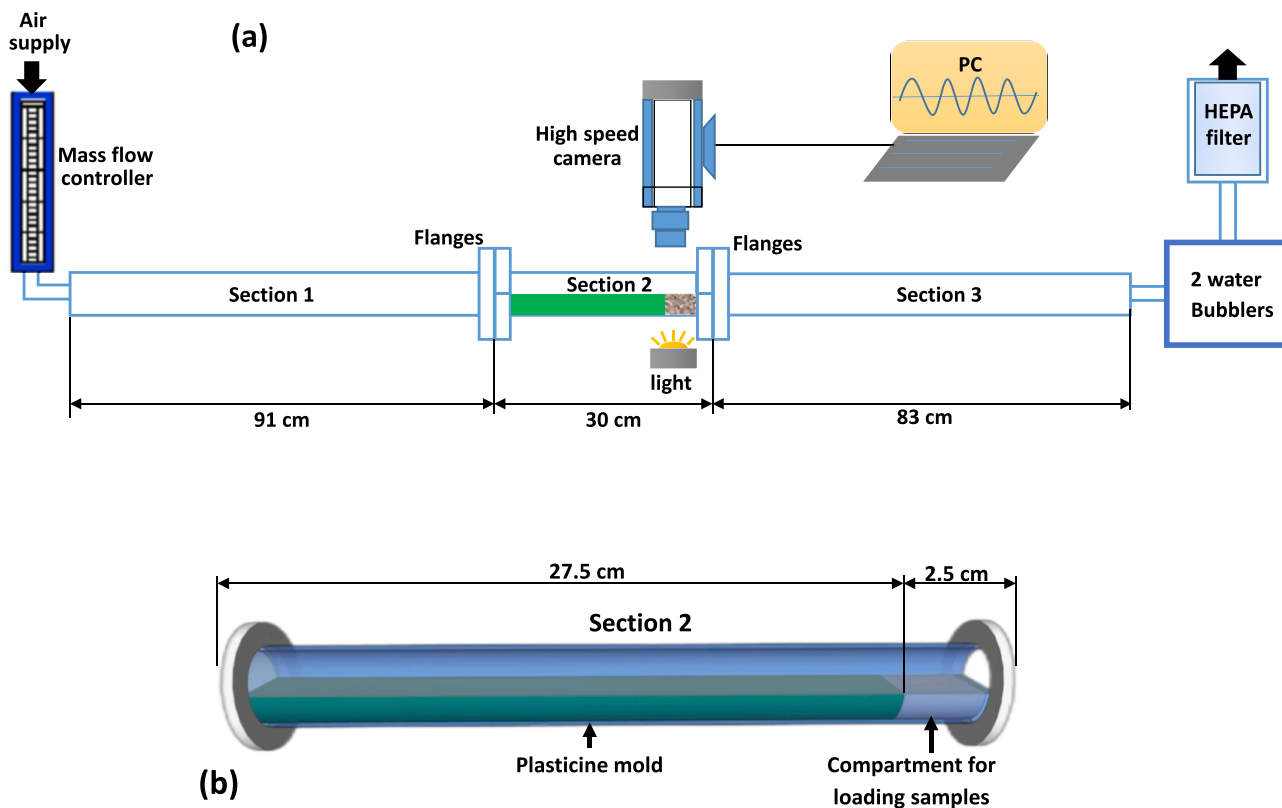

Fig. 1. (a) Schematic of the pneumatic conveying setup; (b) enlarged view of Section 2.

16 mm, made of acrylic, and connected using flanges. The 91 cm long section (1) ensures that the compressed air (purity of 99.99% and water < 5 ppm) fed into the conveying pipeline was fully-developed before entering section (2). The 30 cm long section (2) is comprised of upper and lower semi-cylindrical halves. Specifically, the lower half was packed with plasticine for a length of 27 cm, while a chamber with a length of 2 cm for loading the budesonide samples was to be investigated. Each sample for the pneumatic delivery tests was 0.4 g. The clean & dry compressed air is supplied into section (1) with a maximum flow rate of 0.001 m^3/s controlled by a mass flow controller. The length of section (3) is 83 cm to minimize the exit effects. Two water bubblers and a HEPA filter were used to capture the particles escaping from the pipeline before exhaustion.

The minimum pick-up velocity U_{pu} of uncoated and coated budesonide was determined using the weight-loss method [33,37]. First, the powder sample was loaded into the sample compartment in the lower semi-cylindrical half of section (2), then weighed the apparatus using a four decimal place Mettler Toledo balance. Second, the apparatus was tightly assembled to ensure leakproof. Third, the air was supplied at the desired flow rate for a duration of 60 s. Fourth, the air supply was switched off, the apparatus was dismantled and the bottom half of section (2) was weighed to determine the mass loss. These procedures were repeated at various airflow rates. Three repeat runs at each airflow rate were performed to ensure reproducibility. A high-speed camera with a light source was employed to capture the images of powder samples picked up during pneumatic transportation at a rate of 2000 frames per second. All tests were conducted at room temperature (~20 °C) and with a relative humidity of 47 ± 3 %.

2.6. Atomic force microscopy (AFM) test

Atomic force microscope (AFM) measurements were taken in an NT-MDT (NTEGRA) microscope with OLTESPA silicon nitride cantilevers (Bruker AFM probes) with a stiffness of 2 N/m. The AFM was mounted onto a vibration-isolated table. Small amounts of particles were heaped upon a microscope glass slide, which was then knocked to remove loosely bounded agglomerates. The measurements were performed at ambient conditions, i.e., 20 °C and ~ 40% RH. Particle agglomerates for analysis were selected by a top-view camera mounted on the AFM. Deflection curves (50–200 per sample) were recorded over a 100×100 µm area on several agglomerates to average out local inhomogeneities. Force curves were then obtained by converting the cantilever deflection using Hooke's law and the thermal noise method on a cleaned microscope glass slide. The jumps in the force curves correspond to contacts between two or more particles (see Fig. S1). The contact force between two individual particles was determined by measuring the last jump in the force curves [39–42].

3. Results and discussions

3.1. Morphology of inorganic and organic nanoscale films

Fig. 2 shows TEM images of budesonide particles, uncoated and coated by Al_2O_3, TiO_2, and SiO_2 films via ALD, by poly(ethylene) terephthalate films via MLD and by titanicone films via $TiCl_4$/EG hybrid ALD/MLD. After the deposition processes, fully conformal films were found on the surface of each individual particle. Typically, the thickness of the films deposited via ALD and/or MLD is a few nanometers. Specifically, the average film thicknesses of SiO_2, TiO_2, and titanicone deposited onto budesonide are 1.5 nm, 3 nm, and 4.5 nm after 10 cycles. Al_2O_3 ALD films show instead a higher thickness of ~ 20 nm after 10 cycles due to the infiltration of the TMA precursor into the budesonide particles leading to the formation of an Al_2O_3–budesonide mixed film in the near-surface region [42,43]. In contrast, 50 MLD cycles were required to achieve a 1.5 nm of PET, due to its significantly lower growth per cycle [17].
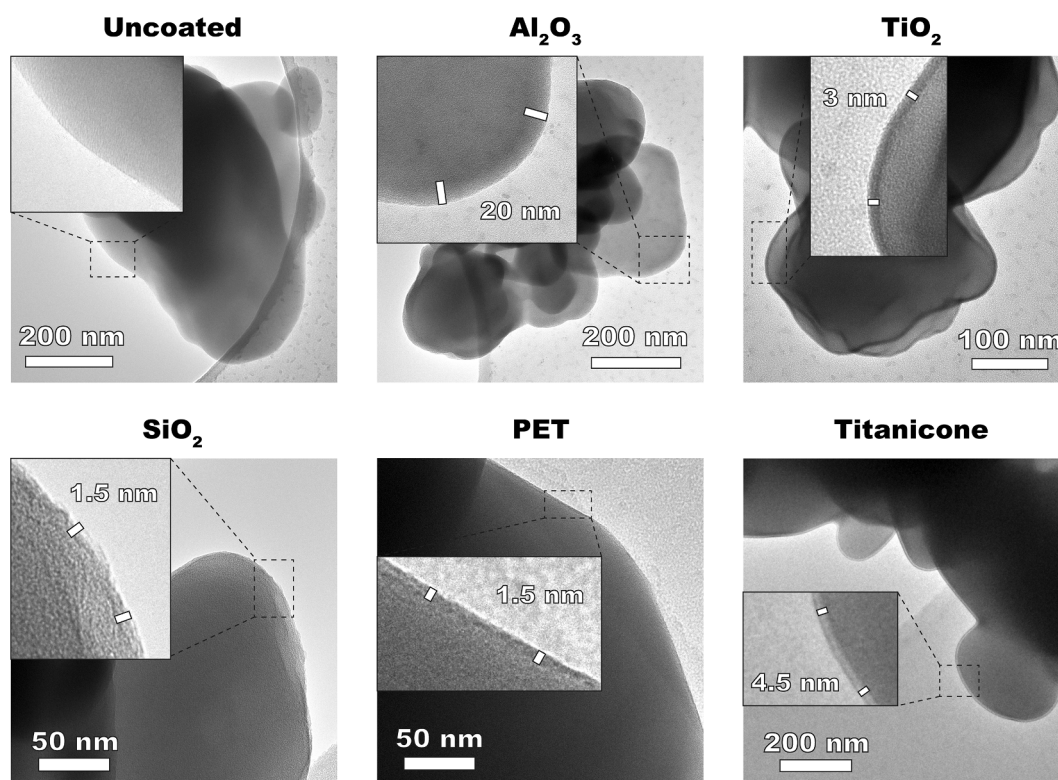

Fig. 2. TEM images of budesonide particles, uncoated and coated by Al_2O_3, TiO_2, and SiO_2 films via ALD, by poly(ethylene) terephthalate films via MLD, and by titanicone films via $TiCl_4$/EG hybrid ALD/MLD. The deposition processes of Al_2O_3, TiO_2, SiO_2, and titanicone were run for 10 cycles, whereas that of PET was for 50 cycles. The details of the experimental conditions are reported in Table 1. The film thicknesses were measured by ImageJ.

3.2. Effect of inorganic and organic nanofilms on flowability

The flowability of the budesonide powders before and after the ALD, hybrid ALD/MLD, and MLD processes were firstly quantified by measuring the static angle of repose (AOR). The AOR represents the angle obtained by forming a cone-like pile of powder when poured onto a flat surface from a set height. Fig. 3 displays the effect of different coating processes, that are the ALD ceramic films, hybrid inorganic/organic ALD/MLD film, and organic MLD film, on the AOR of the budesonide powder. According to the Carr classification [32], powder flowability is categorized as poor, passable, fair, good, and excellent based on the measured AOR. Uncoated budesonide shows poor flowability with an AOR slightly higher than 45°. Instead, an improvement in the flowability performance is achieved after ALD and hybrid ALD/MLD. In particular, titanicone and Al_2O_3 films enhance and render budesonide passable flow, whereas TiO_2 and SiO_2 are fair to flow. The higher AOR measured for Al_2O_3-coated budesonide might be explained by the composition of the surface regions, which include a mixture of budesonide and Al_2O_3. In contrast, PET-coated budesonide exhibits similarly poor flowability to uncoated budesonide. The ALD and hybrid-coated budesonide transform the organic-based surface chemistry into inorganic ones, resulting in a decreased AOR. In contrast, given a sufficiently high cohesivity of the organic (uncoated) budesonide, further depositing organic PET film shows negligible deterioration of flowability.

3.3. Pneumatic delivery behavior

3.3.1. Minimum Pick-up velocity

Pneumatic transportation of budesonide powders is considered similar to the inhalation process of dry drug powders in an inhaler. Drug particles in both scenarios travel in the conveying line, and then experience picked-up, dispersion, and delivery by compressed air. Therefore, pneumatic delivery of budesonide powders can mimic the inhalation (aerosol) behavior, forming a reference to evaluate drug delivery performance. The minimum pick-up velocity (U_{pu}) is the minimum fluid velocity required to mobilize an initially static powder system. The powder particles remain stationary below this velocity but become entrained above. U_{pu}, therefore, excels as an indicator of the powder flowability of ultrafine inhalation drug powders in the conveying line.

Fig. 4 demonstrates the impact on mass loss of both the uncoated and coated budesonide with increasing air velocity. Under the same velocity, a greater amount of powders can be pneumatically delivered for the ALD (TiO_2, SiO_2, and Al_2O_3) and hybrid titanicone coated budesonide

Fig. 3. Comparison of flowability for both uncoated and coated budesonide samples using ALD (TiO_2, SiO_2, Al_2O_3), MLD (PET), and hybrid (titanicone) films. The flowability is characterized by the static angle of repose. A higher static angle of repose indicates worse flowability. The classification is based on the Carr flowability chart [32].

compared to the uncoated or MLD-PET coated ones. This increase in the delivery amount of powders is decreased with an increase in air velocity (*U*). In particular, when picked up by the air velocity at 4.98 m/s, corresponding to a flow rate of 30 L/min as required by the European Pharmacopoeia using a monodose inhaler (RS01, Plastiape) [44] to aerosolize drug powders, more drug powders can be pneumatically transported after organic ALD coatings treatment. The drug delivery (aerosol) performance of inhalation budesonide powders can be beneficial from this improvement in the delivery amount during pneumatic transportation.

Notably, the minimum pick-up velocity U_{pu} of the powder samples tested is determined by extrapolating the two curves shown in Fig. 4 until they intersect the x-axis at which the weight loss is zero, as suggested by [33,38] The value of minimum pickup velocity is reported in Table S2 of the supporting material. Accordingly, Fig. 5 displays the measured U_{pu} for 6 budesonide samples. The results in Fig. 5(a) clearly show that ALD TiO_2 and Hybrid titanicone coated budesonide exhibited lower U_{pu} values than the uncoated or MLD-PET coated budesonide, indicating better flowability. In addition, only a marginal difference in minimum pick-up velocity (U_{pu}) was found for the inorganic ALD coated samples regardless of coating materials (TiO_2, SiO_2, and Al_2O_3), as seen in Fig. 5(b).

3.3.2. Agglomerate formation during pneumatic delivery

High-speed camera imaging revealed the nature of the pick-up behavior of micronized inhalation powders. As shown in Fig. 6, rather than entrained in the form of individual particles with a mean size of 5 μm, the budesonide particles were pneumatically delivered as agglomerates or lumps with a size greater than 100 μm, depending on the coating materials (e.g., organic, inorganic or hybrid). The agglomerate size was estimated using ImageJ software to capture the size information of each particle from the images in Fig. 6. The mean Feret's diameter is used to characterize the average size of agglomerate with irregular shape in this study. The size results of entrained agglomerates for different powder samples are presented in Table S1 (see Supplementary Material). In particular, complex agglomerates, with a medium size of over 500 μm, were observed in the pneumatic transportation of both the uncoated and MLD-PET coated budesonide. This is due to the high cohesivity of the organic surface before coating. On the other hand, the ALD TiO_2 and hybrid titanicone budesonide exhibit improved flowability and dispersibility, as they were transported as much smaller agglomerates, <100 μm for ALD TiO_2 and around 150 μm for hybrid titanicone. Therefore, the growth of inorganic (or component) nanofilm via ALD or Hybrid coating effectively reduced the cohesivity between particles, promoting the flowability.

3.3.3. Re_p* versus Ar plot

The minimum pick-up velocity U_{pu} can be predicted based on the effective Reynolds number (Re_p* which addresses the effect of the pipe diameter) and Archimedes number (*Ar*) according to the well-established Kalman et al. [38] correlation:

$$\text{Zone I}: Re_p^* = 5Ar^{\frac{3}{7}} \quad \text{for} \quad Ar \geqslant 16.5 \tag{1}$$

$$\text{Zone II}: Re_p^* = 16.7 \quad \text{for} \quad 0.45 < Ar < 16.5 \tag{2}$$

$$\text{Zone III}: Re_p^* = 21.8Ar^{\frac{1}{3}} \quad \text{for} \quad Ar \leqslant 0.45 \tag{3}$$

Approximately, Zone I applies to the larger Geldart Group B and D particles, Zone II to Geldart Group A, while Zone III to the highly cohesive Geldart Group C powders [33,34,38,45]. Re_p* and *Ar* are determined as follows:

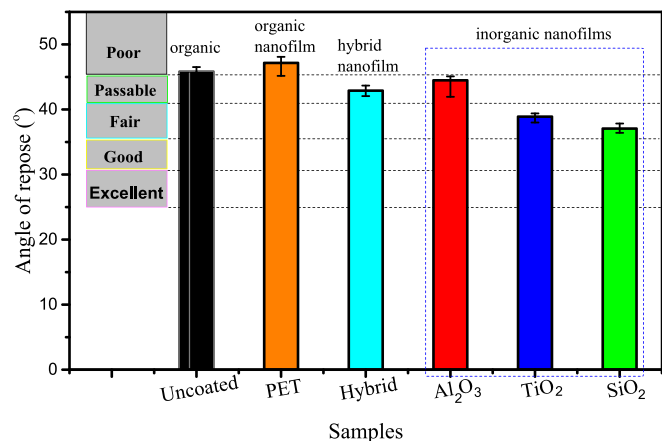$$Re_p^* = \frac{\rho_f d_p U_{pu}}{U_f \left(1.4 - 0.8e^{-\frac{D/D_{ref}}{1.5}}\right)} \tag{4}$$
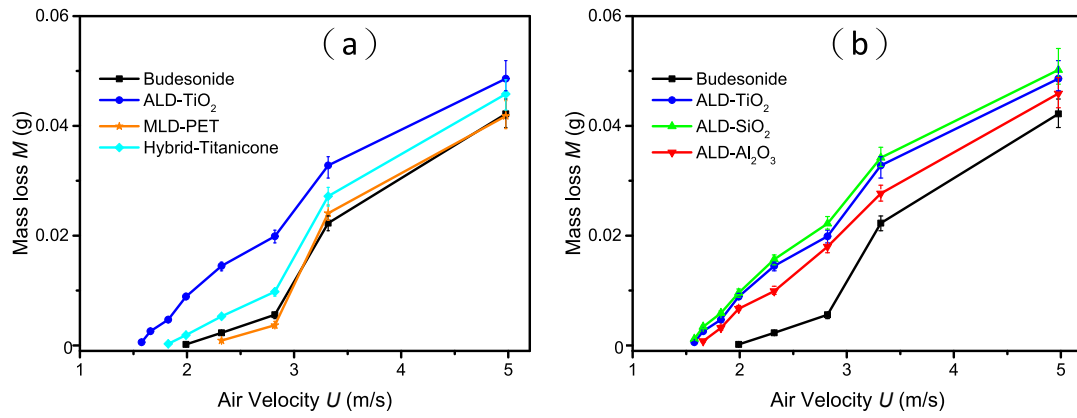
Fig. 4. Mass loss curve of budesonide samples uncoated or coated via ALD, MLD, and hybrid coatings. (a) effect of different coating nanofilms: inorganic (TiO$_2$ coated budesonide), organic (uncoated and PET-coated budesonide), and hybrid organic–inorganic (titanicone coated budesonide); (b) ALD nanofilms with different inorganic materials (TiO$_2$, SiO$_2$, Al$_2$O$_3$).
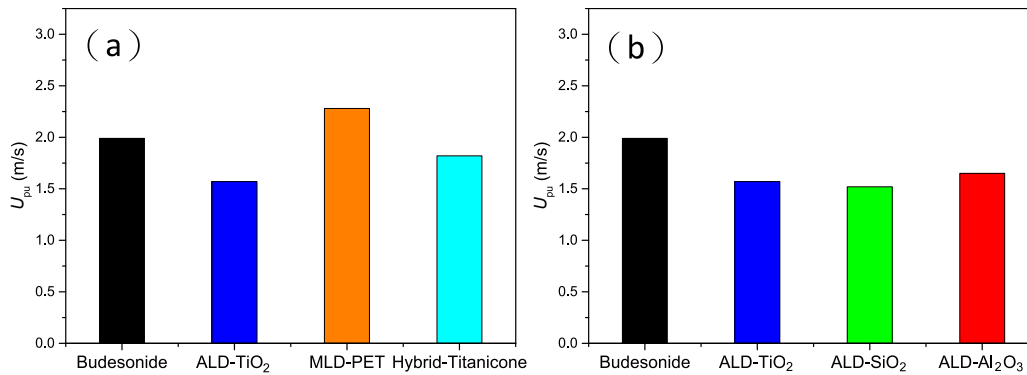

Fig. 5. The minimum pick-up velocity (U_{pu}) is determined by the mass loss curve of budesonide samples uncoated or coated via ALD, MLD, and hybrid coatings. (a) effect of different coating nanofilms: inorganic (TiO$_2$ coated budesonide), organic (uncoated and PET-coated budesonide), and hybrid organic–inorganic (titanicone coated budesonide); (b) ALD nanofilms with different inorganic materials (TiO$_2$, SiO$_2$, Al$_2$O$_3$).
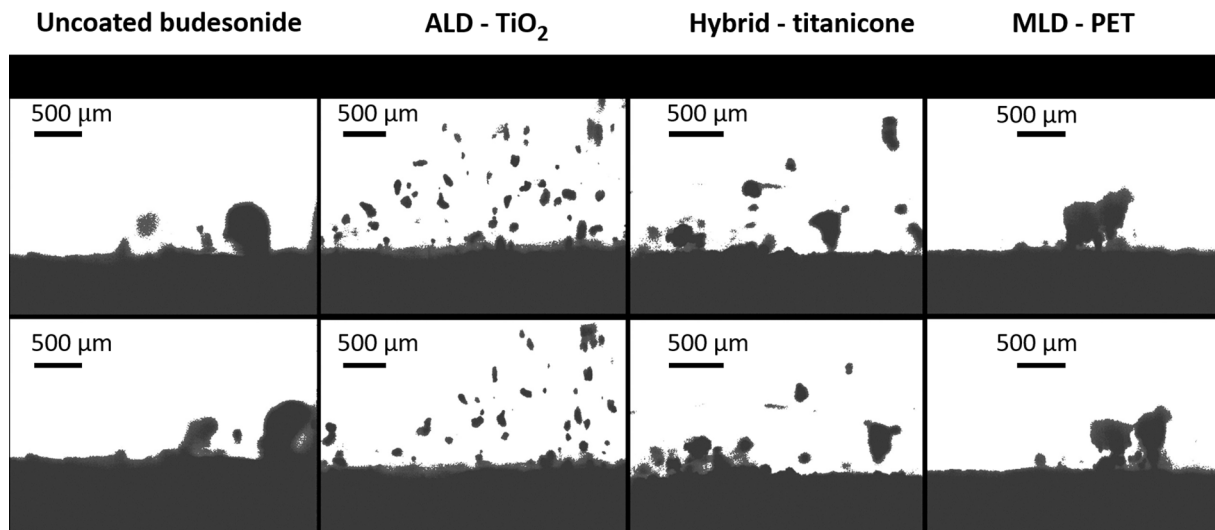

Fig. 6. High-speed camera images at 1 ms interval showing the uncoated and coated budesonide particles being picked up in agglomerates.

$$Ar = \frac{g\rho_f(\rho_p - \rho_f)d_p^3}{\mu_f^2} \quad (5)$$

where ρ_f is the density of air (1.2 kg/m^3), g is the gravitational

acceleration (9.8 m/s^2), μ_f is the air viscosity at ambient conditions (1.81 × 10^{-5} Pa•s), d_p is the particle diameter, D is the pipe diameter (16 mm), D_{ref} is the reference pipe diameter of 50 mm [38,46], and ρ_p is the particle density. The model developed by de Martin and van Ommen (2013) [47] was adopted to estimate the density of the complex

agglomerates (ρ_p) in this work, as seen in Table S1 of the supporting information. More details of the de Martin and van Ommen model predicting the density of fluidized agglomerates can be referred to Ref [47], and the main calculation parameters are similarly used here. Accordingly, the Re_p^* and Ar are calculated and displayed in Table S2 (see Supplementary Material).

Fig. 7 shows the correlation between Re_p^* and Ar, acknowledged for designating the three zones distinguishing three different behaviors in pneumatic conveying systems. The lines represent the correlations, while the discrete points indicate the experimental data obtained in this study. Because of the cohesive nature, Budesonide powders are classified as Geldart Group C particles and should locate in Zone (3) theoretically. The experimentally measured Re_p^* (the star symbol in Fig. 7) was observed at least an order of magnitude lower than the prediction using the Zone (3) correlation. By contrast, the data point of the individual budesonide particle (5 µm diameter) is on the extrapolated line of the extrapolated Zone (1). Similar observations are also found in Ref [33] which focused on the entrainment behavior of nanoparticles. The agglomeration phenomenon witnessed in Fig. 6 can explain the deviation from the predictions by Kalman et al [38] correlation. It should use the agglomerate property (size and density) rather than using that of the individual particle in the calculation. After this correction, it can be seen that no matter the size of agglomerates formed during pneumatic delivery, all tested samples (data points in Fig. 7) were well represented by the Zone (1) correlation, showing the flow behavior of Geldart group B particles.

3.3.4. Minimum pick-up velocity (U_{pu}) v.s. inter-particle forces(F)

Fig. 8 shows the relationship between the inter-particle force (F) obtained by AFM tests and the minimum pick-up velocity (U_{pu}) of different powder samples. The measured U_{pu} is observed generally proportional to F. The ALD-coated budesonide indeed shows reduced inter-particle force compared to the uncoated budesonide, which explains the earlier discussed enhanced flowability. The PET-coated budesonide exhibits large interparticle forces, explaining the poor flowability similar to the uncoated budesonide. The hybrid coated budesonide indeed has an intermediate value for the inter-particle forces, in line with its passable flow performance.
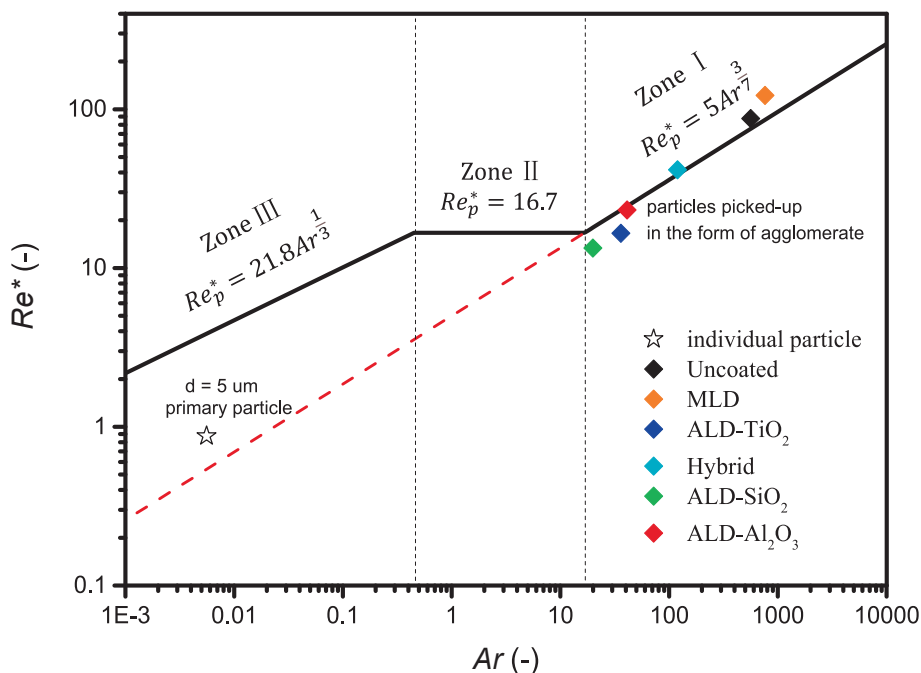

Fig. 8. Correlation between minimum pick-up velocity (U_{pu}) and interparticle force of uncoated and coated budesonide with different coating films (inorganic, organic, and hybrid). The error bars indicate standard deviations.

The flow characteristics of powders depend on both the chemical composition and physical structure (surface roughness/morphology), which are particularly in relation to adhesion, friction, and flow. ALD/MLD coating only generates nanoscale films on the surface of individual particles. This conformal nano-film shows high shape retention. Therefore, we expect insignificant influences on the physical structure of the original budesonide particle. The reason why depositing different materials via ALD/MLD can effectively alter the flowability of budesonide powders is mainly due to the change in the chemical composition of the surface of the budesonide particles after coating.

The Hamaker constant, A_H, is commonly used to evaluate the interaction force between the fine particles. Metals and metal oxides (inorganic materials) in general have different Hamaker constants than organic materials [48–51], therefore, the surface chemistry can significantly influence the surface connectivity. The inorganic nanofilms

Fig. 7. Re_p^* versus Ar plot. The solid line represents the correlations for each zone, the dashed line represents the extrapolated Zone 1 correlation, while each discrete data point represents the different powder samples investigated Specifically, Zones 1, 2, and 3 approximately correspond to Geldart groups B, A, and C, respectively.
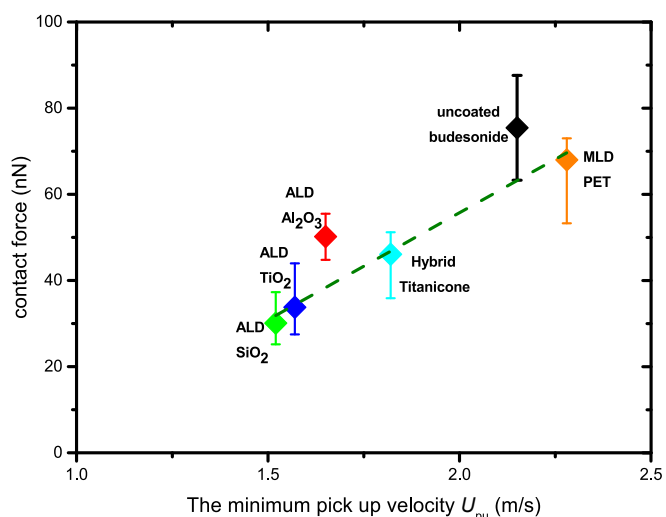
deposited onto the budesonide particles, such as SiO_2 ($A_H = 7.2 \times 10^{-20}$), Al_2O_3 ($A_H = 1.45 \times 10^{-19}$) and TiO_2 ($A_H = 1.54 \times 10^{-19}$) [52], give much smaller Hamaker constants (or surface energy) than uncoated budesonide ($A_H = 5 \times 10^{-19}$) [53]. The inorganic films obtained via ALD reduce the inter-particle interactions validated by the AFM measurements, resulting in a better performance in flow behavior. Instead, the organic PET films coated via MLD have a comparable Hamaker constant with the uncoated budesonide. From the correlation in [51], we can calculate $A_H = 7 \times 10^{-19}$, but this is a rough estimate: the correlation has a certain error and the PET film by MLD is likely to deviate from bulk PET. Thus, they show similarly poor flow behavior. For the titanicone, no Hamaker constant could be found in the literature, but it is expected to be between that of the budesonide and ceramic materials.

4. Conclusions

In this study, we have explored the effect of surface modification on individual particles via ALD/MLD coatings on the flow characteristics of pharmaceutical powders (low micron-sized powders, <30 μm, with a special focus on 2–5 μm particles) for inhaled drug delivery. The flow properties are characterized by the angle of repose (static) and pneumatic delivery (dynamic) tests, which can evaluate the drug delivery performance of drug inhalation. Depositing different materials (organic, inorganic, and hybrid) in the form of nanofilms onto the host drug particles can effectively alter the flow behavior. In particular, the growth of inorganic nanofilm (SiO_2, TiO_2, or Al_2O_3) via ALD and hybrid nanofilm (titanicone) via combined ALD-MLD coating not only decreases the angle of repose and minimum pick-up velocity (U_{pu}) but also promote the pneumatic delivery of a much higher amount of drug powders. Instead, the uncoated and organic PET coated budesonide show comparably poor flowability. Due to the high cohesivity, the uncoated and MLD-PET coated budesonide are pneumatically transported in large (complex agglomerate) clusters with a medium size of over 500 μm. The good flow is achieved both for ALD and hybrid coated budesonide reflected by a considerable decrease in the size of agglomerate during pick-up. This improvement is attributed to the reduction of the interparticle force between drug particles by the inorganic or hybrid nanofilms as confirmed through the AFM measurements.

Knowledge gained from this study connects several 'key powder material length scales' that provide a basis for a more mechanistic understanding of dry particle surface modification on bulk powder functionality. Moreover, this flow modification method via ALD/MLD coatings at the nanoscale, not only can be used for pharmaceutical applications but can benefit other powder processing industries, such as food, cosmetics, energy, additive manufacturing, and catalysts.

Declaration of Competing Interest

The authors declare that they have no known competing financial interests or personal relationships that could have appeared to influence the work reported in this paper.

Data availability

Data will be made available on request.

Acknowledgments

Appendix A. Supplementary data

Supplementary data to this article can be found online at https://doi.org/10.1016/j.cej.2023.142131.

References

[1] J.K. Prescott, R.A. Barnum, On powder flowability, Pharm. Technol. 24 (10) (2000) 60–85.

[2] Q.T. Zhou, B. Armstrong, I. Larson, P.J. Stewart, D.A. Morton, Understanding the influence of powder flowability, fluidization and de-agglomeration characteristics on the aerosolization of powder model powders, Eur. J. Pharm. Sci. 40 (5) (2010) 412–421.

[3] B. Chaurasiya, Y.Y. Zhao, Dry powder for pulmonary delivery: A comprehensive review, Pharmaceutics 13 (1) (2020) 31.

[4] L.J. Jallo, C. Ghoroi, L. Gurumurthy, U. Patel, R.N. Davé, Improvement of flow and bulk density of pharmaceutical powders using surface modification, Int. J. Pharm. 423 (2) (2012) 213–225.

[5] R. Gannoun, J.M.P. Ebri, A.T. Perez, M.J. Espin, F.J. Duran-Olivencia, J. M. Valverde, Nanosilica to improve the flowability of fine limestone powders in thermochemical storage units, Chem. Eng. J. 426 (2021).

[6] R. Gannoun, F.J. Durán-Olivencia, A.T. Pérez, J.M. Valverde, Titania coatings: A mechanical shield for cohesive granular media at high temperatures, Chem. Eng. J. 450 (2022) 138123.

[7] R. Beetstra, U. Lafont, J. Nijenhuis, E.M. Kelder, J.R. van Ommen, Atmospheric pressure process for coating particles using atomic layer deposition, Chem. Vap. Depos. 15 (7–9) (2009) 227–233.

[8] R.W. Johnson, A. Hultqvist, S.F. Bent, A brief review of atomic layer deposition: from fundamentals to applications, Mater. Today 17 (5) (2014) 236–246.

[9] J.R. van Ommen, A. Goulas, Atomic layer deposition on particulate materials, Mater. Today Chem. 14 (2019).

[10] C. Hirschberg, N.S. Jensen, J. Boetker, A.Ø. Madsen, T.O. Kääriäinen, M.- L. Kääriäinen, P. Hoppu, S.M. George, M. Murtomaa, C.C. Sun, J. Risbo, J. Rantanen, Improving powder characteristics by surface modification using atomic layer deposition, Org. Process Res. Dev. 23 (11) (2019) 2362–2368.

[11] A.W. Weimer, Particle atomic layer deposition, J. Nanopart. Res. 21 (1) (2019) 9.

[12] D.M. King, X. Liang, A.W. Weimer, Functionalization of fine particles using atomic and molecular layer deposition, ECS Trans. 25 (4) (2009) 163–190.

[13] J. Liu, A. Wei, G. Pan, Q. Xiong, F. Chen, S. Shen, X. Xia, Atomic layer deposition-assisted construction of binder-free Ni@ N-doped carbon nanospheres films as advanced host for sulfur cathode, Nano-Micro Letters 11 (1) (2019) 1–14.

[14] D. La Zara, M.R. Bailey, P.L. Hagedoorn, D. Benz, M.J. Quayle, S. Folestad, J.R. van Ommen, Sub-nanoscale surface engineering of TiO2 nanoparticles by molecular layer deposition of poly (ethylene terephthalate) for suppressing photoactivity and enhancing dispersibility, ACS Appl. Nano Mater. 3 (7) (2020) 6737–6748.

[15] T.O. Kääriäinen, M. Kemell, M. Vehkamäki, M.-L. Kääriäinen, A. Correia, H. A. Santos, L.M. Bimbo, J. Hirvonen, P. Hoppu, S.M. George, D.C. Cameron, M. Ritala, M. Leskelä, Surface modification of acetaminophen particles by atomic layer deposition, Int. J. Pharm. 525 (1) (2017) 160–174.

[16] D. Zhang, D. La Zara, M.J. Quayle, G. Petersson, J.R. van Ommen, S. Folestad, Nanoengineering of crystal and amorphous surfaces of pharmaceutical particles for biomedical applications, ACS Applied Bio Materials 2 (4) (2019) 1518–1530.

[17] D. La Zara, F. Zhang, F. Sun, M.R. Bailey, M.J. Quayle, G. Petersson, S. Folestad, J. R. van Ommen, Drug powders with tunable wettability by atomic and molecular layer deposition: From highly hydrophilic to superhydrophobic, Appl. Mater. Today 22 (2021).

[18] D.H.K. Jackson, B.J. O'Neill, J. Lee, G.W. Huber, J.A. Dumesic, T.F. Kuech, Tuning Acid–base properties using Mg–Al oxide atomic layer deposition, ACS Appl. Mater. Interfaces 7 (30) (2015) 16573–16580.

[19] L.F. Hakim, D.M. King, Y. Zhou, C.J. Gump, S.M. George, A.W. Weimer, Nanoparticle coating for advanced optical, mechanical and rheological properties, Adv. Funct. Mater. 17 (16) (2007) 3175–3181.

[20] J. Guo, D. Benz, T.T.D. Nguyen, P.H. Nguyen, T.L.T. Le, H.H. Nguyen, D. La Zara, B. Liang, H.T.B. Hintzen, J.R. van Ommen, H. Van Bui, Tuning the photocatalytic activity of TiO2 nanoparticles by ultrathin SiO2 films grown by low-temperature atmospheric pressure atomic layer deposition, Appl. Surface Sci. 530 (2020).

[21] J. Miller, C. Gillespie, J. Chesser, A. Scheppe, T. Bryson, J. Dixon, A. Nelson, N. Teslich, A. Lange, S. Elhadj, R.V. Reeves, Surface modification of organic powders for enhanced rheology via atomic layer deposition, Adv. Powder Technol. 31 (6) (2020) 2521–2529.

[22] M. Shimel, I. Gouzman, E. Grossman, Z. Barkay, S. Katz, A. Bolker, N. Eliaz, R. Verker, Enhancement of wetting and mechanical properties of UHMWPE-based composites through alumina atomic layer deposition, Adv. Mater. Interfaces 5 (14) (2018) 1800295.

[23] J. Malm, E. Sahramo, M. Karppinen, R.H. Ras, Photo-controlled wettability switching by conformal coating of nanoscale topographies with ultrathin oxide films, Chem. Mater. 22 (11) (2010) 3349–3352.

[24] J. Bae, I.A. Samek, P.C. Stair, R.Q. Snurr, Investigation of the Hydrophobic Nature of Metal Oxide Surfaces Created by Atomic Layer Deposition, Langmuir 35 (17) (2019) 5762–5769.

[25] S. Gupta, M. Mittal, A.S. Rathore, Atomic Layer Deposition Coating on the Surface of Active Pharmaceutical Ingredients to Reduce Surface Charge Build-Up, ACS Appl. Mater. Interfaces 14 (23) (2022) 27195–27202.

[26] S.M. George, B. Yoon, A.A. Dameron, Surface chemistry for molecular layer deposition of organic and hybrid organic-inorganic polymers, Acc. Chem. Res. 42 (4) (2009) 498–508.

[27] A.G. Carr, R. Mammucari, N.R. Foster, Particle formation of budesonide from alcohol-modified subcritical water solutions, Int. J. Pharm. 405 (1–2) (2011) 169–180.

[28] L.M. Nolan, L. Tajber, B.F. McDonald, A.S. Barham, O.I. Corrigan, A.M. Healy, Excipient-free nanoporous microparticles of budesonide for pulmonary delivery, Eur. J. Pharm. Sci. 37 (5) (2009) 593–602.

[29] T. Rattanupatam, T. Srichana, Budesonide dry powder for inhalation: effects of leucine and mannitol on the efficiency of delivery, Drug Deliv. 21 (6) (2014) 397–405.

[30] D. Geldart, E.C. Abdullah, A. Hassanpour, L.C. Nwoke, I.J.C.P. Wouters, Characterization of powder flowability using measurement of angle of repose, China Particuology 4 (3–4) (2006) 104–107.

[31] M. Krantz, H. Zhang, J. Zhu, Characterization of powder flow: Static and dynamic testing, Powder Technol. 194 (3) (2009) 239–245.

[32] H.M.B. Al-Hashemi, O.S. B. Al-Amoudi, A review on the angle of repose of granular materials, Powder Technol 330 (2018) 397–417.

[33] A. Anantharaman, J.R. van Ommen, J.W. Chew, Minimum pick-up velocity (U_{pu}) of nanoparticles in gas–solid pneumatic conveying, J. Nanopart. Res. 17 (12) (2015) 1–10.

[34] A. Anantharaman, J.R. van Ommen, J.W. Chew, Minimum pick-up velocity: The transition between nano-scale and micro-scale, AIChE J 63 (5) (2017) 1512–1519.

[35] A. Anantharaman, A. Cahyadi, K. Hadinoto, J.W. Chew, Impact of particle diameter, density and sphericity on minimum pick-up velocity of binary mixtures in gas-solid pneumatic conveying, Powder Technol. 297 (2016) 311–319.

[36] A. Anantharaman, X. Wu, K. Hadinoto, J.W. Chew, Impact of continuous particle size distribution width and particle sphericity on minimum pick-up velocity in gas–solid pneumatic conveying, Chem. Eng. Sci. 130 (2015) 92–100.

[37] Y. Zhao, S. Dahiphale, Y.Z. Tan, C.H. Wang, J.W. Chew, The effect of particle initial charge on minimum pick-up velocity (U_{pu}) in pneumatic conveying, Chem. Eng. Res. Des. 156 (2020) 343–352.

[38] H. Kalman, A. Satran, D. Meir, E. Rabinovich, Pick-up (critical) velocity of particles, Powder Technol. 160 (2) (2005) 103–113.

[39] X. Yu, S.M. Hörst, C. He, P. McGuiggan, N.T. Bridges, Direct measurement of interparticle forces of Titan aerosol analogs ("tholin") using atomic force microscopy, J. Geophys. Res. Planets 122 (12) (2017) 2610–2622.

[40] S. Salameh, J. Schneider, J. Laube, A. Alessandrini, P. Facci, J.W. Seo, L.C. Ciacchi, L. Madler, Adhesion mechanisms of the contact interface of TiO2 nanoparticles in films and aggregates, Langmuir 28 (2012) 11457–11464.

[41] S. Salameh, R. Scholz, J.W. Seo, L. Madler, Contact behavior of size fractionated TiO2 nanoparticle agglomerates and aggregates, Powder Technol. 256 (2014) 345–351.

[42] D. La Zara, F. Sun, F. Zhang, F. Franek, K. Balogh Sivars, J. Horndahl, S. Bates, M. Brännström, P. Ewing, M.J. Quayle, G. Petersson, S. Folestad, J.R. van Ommen, Controlled pulmonary delivery of carrier-free budesonide dry powder by atomic layer deposition, ACS Nano 15 (4) (2021) 6684–6698.

[43] J.W. Elam, J.A. Libera, T.H. Huynh, H. Feng, M.J. Pellin, Atomic layer deposition of aluminum oxide in mesoporous silica gel, J. Phys. Chem. C 114 (41) (2010) 17286–17292.

[44] F. Lavorini, M. Pistolesi, O.S. Usmani, Recent advances in capsule-based dry powder inhaler technology, Multidiscip. Respirat. Med. 12 (1) (2017) 1–7.

[45] D. Geldart, Types of gas fluidization, Powder Technol. 7 (5) (1973) 285–292.

[46] J.Y.T. Tay, J.W. Chew, K. Hadinoto, Analyzing the minimum entrainment velocity of ternary particle mixtures in horizontal pneumatic transport, Ind. Eng. Chem. Res. 51 (15) (2012) 5626–5632.

[47] L. de Martín, J.R. van Ommen, A model to estimate the size of nanoparticle agglomerates in gas− solid fluidized beds, J. Nanopart. Res. 15 (11) (2013) 1–9.

[48] L. Bergström, Hamaker constants of inorganic materials, Adv. Colloid Interface Sci. 70 (1997) 125–169.

[49] J.S. Marshall, S. Li. Adhesive Particle Flows, Cambridge University Press, 2014, pp. 81–129.

[50] T. Zhou, H. Li, Estimation of agglomerate size for cohesive particles during fluidization, Powder Technol. 101 (1) (1999) 57–62.

[51] H. Takagishi, T. Masuda, T. Shimoda, R. Maezono, K. Hongo, Method for the calculation of the hamaker constants of organic materials by the lifshitz macroscopic approach with density functional theory, Chem. A Eur. J. 123 (40) (2019) 8726–8733.

[52] M. Tahmasebpoor, L. de Martín, M. Talebi, N. Mostoufi, J.R. van Ommen, The role of the hydrogen bond in dense nanoparticle–gas suspensions, PCCP 15 (16) (2013) 5788–5793.

[53] B. van Wachem, K. Thalberg, J. Remmelgas, I. Niklasson-Björn, Simulation of dry powder inhalers: combining micro-scale, meso-scale and macro-scale modeling, AIChE J. 63 (2) (2017) 501–516.